Thermocouple-based thermometry for laminar sooting flames: Implementation of a fast and simple methodology

Jessy Elias, Alessandro Faccinetto, Sebastien Batut, Olivier Carrivain, Mariano Sirignano, Andrea d'Anna, Xavier Mercier

Thermocouple-based thermometry for laminar sooting flames: Implementation of a fast and simple methodology

Jessy Elias[a,b], Alessandro Faccinetto[a], Sebastien Batut[a], Olivier Carrivain[a], Mariano Sirignano[c], Andrea D'Anna[c], Xavier Mercier[a,*]

[a] *Univ. Lille, CNRS, UMR 8522, PC2A, Villeneuve d'Ascq, France*

[b] *French Environment and Energy Management Agency, Angers, France*

[c] *Univ. Napoli Federico II, Dipartimento di Ingegneria Chimica, dei Materiali e della Produzione Industriale, Napoli, Italy*

*Corresponding author

Abstract

This work reports the implementation and the validation of the extrapolation method for thermocouple temperature measurements corrected from the radiation losses in sooting flames. This simple method relies on the use of a few thermocouples having different size diameters enabling a fast and direct determination of the flame temperature by extrapolation to zero diameter. We propose here a detailed study of the possibilities and limitations provided by this method based on experimental measurements and comparison with well-established methods carried out in a laminar diffusion sooting flame. In this work, a specific fast insertion setup involving four different sized thermocouples has been implemented to record temperature values at different heights in the flame. From these data, we highlight that a linear calibration curve correlated the raw measured temperatures to the flame temperatures corrected from the radiation loss can be easily and rapidly obtained. The impact of soot on the temperature measurement is also discussed. To assess the reported thermocouple methodology, a direct comparison is made between the temperature profile determined along the vertical central axis of the flame by the extrapolation method with OH and NO LIF thermometry measurements as well as numerical simulation. Finally, we also report comparisons of experimental and simulated radial temperature profiles highlighting the suitable dynamic of the method for temperature profile determination in high temperature gradient conditions (500 K/mm). This work demonstrates that the extrapolation method appears as an efficient and fast method to determine accurate temperature profiles in flames, even in presence of soot particles, which might be further simplified to help the development of fast and cheap sensors for either laboratory or larger-scale applications.

Keywords: Thermometric Sensors, Flame temperature; Thermocouple methodology; Extrapolation method; Radiative loss correction

1. Introduction

Temperature measurements are crucial in the context of laboratory flame studies for the development and validation of detailed kinetic models[1]. These measurements are usually performed by optical methods or thermocouple thermometry. Optical methods have the great advantage of being non-intrusive, thus allowing local measurements without disturbance of the flame[2]. In that context, methods such the line-of-sight attenuation (LOSA) [3,4] and spectral soot emission (SSE) [5] are relatively easy to implement and give access to integrated temperature measurements requiring nevertheless complex inversion procedures to recover the temperature mapping of the flame. Moreover, these methods are dependent on the presence of soot particles, being therefore only applicable to sooting flames and providing temperature information restricted to the region where soot are formed. Laser-induced fluorescence (LIF) and coherent anti-stokes Raman scattering (CARS) are certainly the most commonly used methods for the determination of temperatures in flames[2]. LIF is based on the excitation of species, usually radicals, formed in the flame (e.g. OH or NO) and the recording of their rovibronic excitation spectra over a certain collection wavelength range[6–9]. Being the intensity of the lines proportional to the Boltzmann factor, the temperature of the flame can be obtained by comparison with simulated spectra. LIF, which is widely used in laboratory flames[10], with satisfying accuracy (less than 100 K uncertainty). CARS is probably the optical method offering the highest accuracy (less than 50 K uncertainty)[11] for flame temperature measurements. However, this method relies on complex non-linear optics and requires a delicate experimental implementation, in particular the crossing of several laser beams at the temperature measurement point which noticeably limit the spatial resolution of this technique.

Compared to optical techniques, thermocouple-based temperature measurements require much less expensive equipment and appear much simpler to implement. A thermocouple consists of two different metal alloy wires, joined at one end. When the junction of the two metals is heated, a voltage is produced at open ends that can be correlated back to the junction temperature. Unlike optical measurements, the use of thermocouples necessarily results in a disturbance of the investigated medium as the junction needs to be physically located at the temperature measurement point. In addition, thermocouple-based measurements in combustion environments require some corrections to retrieve the flame temperature that include the effect of losses by heat conduction, convection and thermal radiation[1]. Thermocouple measurements can also be biased by catalytic oxidation processes likely to occur at the surface of the alloys, in particular under the action of H or OH radicals in flames[12]. Many works have been searching methods for mitigation of the impact of all these phenomena on temperature measurements [1,5,13–15]. It is notably recommended to allow single temperature measurements that the Biot number characterizing the heating uniformity of the junction should be well below 0.1[1]. Measurement biases related to conduction can also be greatly reduced by

selecting thermocouples having a wire length/diameter ratio greater than 200[12,13]. Finally, surface coatings with beryllium or yttrium oxide are known to limit catalytic oxidation[16,17].

The radiative losses, which are inherent to the heating of the thermocouple and thus cannot be completely avoided, can lead to underestimation of the flame temperature by several hundreds of degrees in high temperature media[5]. Also, if present, soot can deposit on the junction, significantly changing its diameter and emissivity. Even though thermocouples can be used to estimate the soot amount in flame by thermophoretic particle densitometry (TPD)[18–20], reliable temperature measurements in sooting flames are still challenging. In a recent paper, Lemaire et al.[15] proposed a comparative study of 4 different thermocouple methods relying on different corrections processes, namely the electrical compensation (EC), the reduced radiative error (RRE), the multi-element methods (MET) and the extrapolation method. In this work, the authors have made a detailed study relating the implementation of the methods along with a comparison of their sensitivity and accuracy relative to each other. The EC method consists of heating the thermocouple in a vacuum by imposing a high frequency alternating current and measuring the DC electromotive force at the terminals of the thermocouple. In vacuum, since there is no external energy input through gases, the electrical energy supplied per unit length to the thermocouple is equal to the heat loss by radiation. Hence, a first calibration curve is obtained in vacuum condition characterizing the temperature reached by the thermocouple according to the applied current. The thermocouple is then placed at different heights in the flame and by applying the same procedure as in vacuum, it is possible to deduce by comparison with the initial calibration curve the losses by radiation as a function of the measured temperature. Hence, the EC method, although very accurate, requires expensive equipment (ultra-high vacuum cell to determine the radiation losses) and a relatively long and complex implementation which can represent a limitation to its use for flame studies. The RRE method[15]which aims to evaluate by calculation the radiative losses requires knowledge or estimates of the parameters of the studied medium (viscosity, density, flow velocity, gas environment....) which can be difficult to determine and thus might also appear to a limitation for the use of this method. The MET method, which is based on the use of a simple analytical expression to find the true temperature using two or three thermocouples of different diameters, has been shown to often give inconsistent results, as also noted elsewhere[14,15]. The reason might be related to the terms in T^4 in the used expression, being too sensitive to temperature variations. Finally, the extrapolation method, assuming the radiative losses to be proportional to the diameter of the thermocouple[13,21,22], requires only simple equipment and no a priori knowledge on the combustion medium to retrieve flame temperature. Thus, by making measurements with thermocouples of different diameters, the flame temperature can be deduced by extrapolation to the zero diameter. Besides, the use of thermocouple with two different bead sizes can also be judiciously used to determine the radiation correction for the gas temperature in a steady flames by solving a simple energy balance equation[23,24]. In the paper of Lemaire[15], the result of the extrapolation

method implemented with only two measurement points corresponding to two thermocouples of different diameters is compared with the three other methods (EC, RRE and MET). The good agreement obtained by linear extrapolation with the results of the EC and RRE methods appears to be satisfactory. These preliminary results suggest that the use of the extrapolation method with more measurement points could therefore allow obtaining temperature measurements corrected for radiative losses with a high degree of accuracy. However, despite being one of the oldest documented methods in modern combustion science[18], systematic studies aiming to validate the use of this simple-to-implement and inexpensive method for the measurement of temperature profiles in flames are scarce in the literature[13,14,21,22,25]. Moreover, there exist some discrepancies between the published works on the analytical treatment of the data to recover flame temperature. To address this lack of consistency, we propose herein to test the possibilities and limitations offered by the extrapolation method for the measurement of temperature profiles corrected from radiation losses in sooting flames. This work is carried out in a well-characterized laminar diffusion flame[26,27] and explains in details the principle and the methodology to implement the extrapolation method to sooting flames. A validation of the method is proposed based on the comparison with temperature measurements performed by laser based techniques like OH and NO LIF thermometry and numerical simulations. Finally, a discussion on the measurement biases potentially occurring due to the presence of soot is proposed.

2. Experimental Setup

2.1 Burner and flame apparatus

Measurements were performed along the axis of a 120 mm height, non-smoking, laminar diffusion flame (0.52 L min^{-1} CH_4, 87 L min^{-1} air) stabilized at atmospheric pressure on a modified McKenna burner with a central injector tube (10.25 mm diameter) and an outer air flow tube (88 mm diameter) producing a homogenous air shield. This flame has already been characterized in previous works[26,27]. In particular, laser induced incandescence (LII) measurements showed that soot particles along the vertical central axis of the flame are located between 55 and 100 mm height above the burner (HAB), with a peak volume fraction at 80 mm HAB.

2.2 LIF thermometry

OH and NO LIF thermometry are well-established experimental optical techniques that were used as reference methods for validating the temperature profile measurement. The flame was not doped, so the temperature measurements were limited to the HABs providing a sufficient concentration of OH and NO radicals for the recording of the excitation spectra. Hence, NO LIF thermometry was preferentially used for

the lowest HABs up to 40 mm, while OH LIF thermometry could only be used above 80 mm HAB, in the oxidation zone of the flame.

OH and NO LIF thermometry measurements were carried out with a Nd:YAG laser (Quanta-ray, Spectra Physics), generating laser pulses at 1064, 532 and 355 nm (6 ns pulse width, 10 Hz) mixed and used to pump an OPO (premiScan-ULD/240, GWU-Lasertechnik) with tunable wavelengths in a large spectral range from the UV to the IR. Two different optical schemes were used according to the excited species. In both cases, the laser beam was focused on the flame axis using a spherical UV lens (1000 mm focal length). The laser beam diameter at the probed volume was estimated to be around 500 μm. The laser fluence was kept below 20 mJ cm^{-2} with an optical attenuator to be in the linear regime of fluorescence.

NO LIF experiments were carried out by exciting NO lines in the A-X (0–0) band system around 226 nm. The emitted fluorescence was collected at a right angle in the (0–2) band around 245 nm with two spherical lenses (50 mm diameter, 100 and 75 mm focal length, respectively) and imaged into a bundle of optical fibers (1.25 mm diameter) connected to a spectrometer (IHR320, Jobin Yvon) coupled to a photomultiplier tube (XP2020Q, Photonics). With this spectroscopic scheme, no spectral interference or overlap with aromatic hydrocarbons fluorescence was reported. Finally, the spectral comparison between experimental and simulated spectra did not consider quenching variations as the fluorescence quenching of NO has been demonstrated to be insensitive to the rotational quantum number[28–30], making these species highly recommended for temperature profile determination in flames.

OH LIF spectra were obtained by using a tunable excitation wavelength in the A-X (0-0) band from 309 to 312 nm and by collecting the fluorescence signal in the (0-0) band in the spectral range 305-308 nm corresponding to the R bands. The anti-Stokes collection scheme was necessary to minimize potential spectral interferences with the intense fluorescence of polycyclic aromatic hydrocarbons (PAHs) above 300 nm[27]. Except the selected fluorescence spectral range, the whole collection system (optics and detectors) was identical to the one used for the NO LIF experiments. Again, based on previous works on OH LIF thermometry[7,31–33], no quenching variations were considered here. Measurements were obtained promptly after the laser pulse to minimize the effect of quantum yield variations with rotational levels as recommended in the literature, showing that in this case, rotational level-dependences of radiative and quenching rates almost canceled and the error became negligible. The uncertainty reported in the present paper (~160 K at 1750K) corresponds the estimated errors between the fit of the experimental and simulated spectrum[34].

The spectrometer was wavelength-calibrated using the spectral lines of a mercury pen lamp.

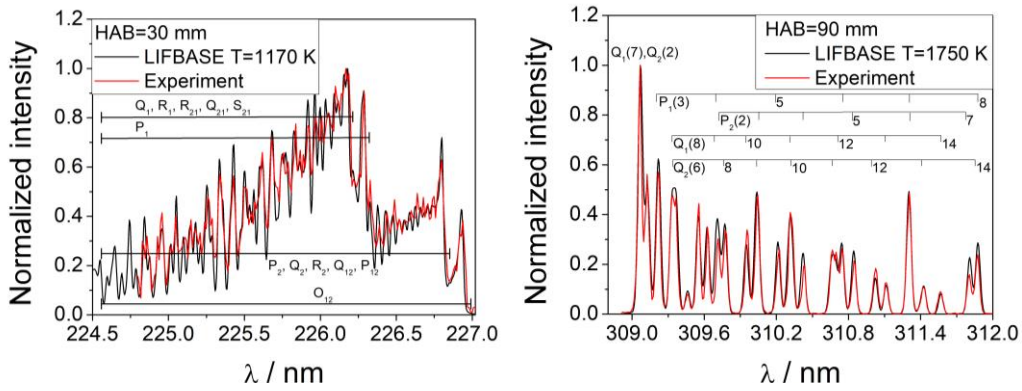

Fig.1 Determination of the temperature by LIF NO (left panel) and LIF OH (right panel) for different HABs.

The flame temperature was determined from the comparison of the experimental spectra with simulations (LIFBASE software) performed by adjusting the temperature parameter to obtain the best match between the experimental and simulated spectra. Two examples with both OH and NO spectra determined for different HABs are reported in fig.1. From the statistical error in the Boltzmann plots, the temperature uncertainties were estimated around ±80K and ±100K respectively for OH and NO LIF measurements[9].

2.3 Flame temperature simulations

Numerical simulations were performed in order to predict the flame temperature by using a detailed kinetic mechanism for hydrocarbon oxidation and pyrolysis, able to model several premixed and diffusion flames at atmospheric pressure[19,35–38]. In the mechanism, benzene formation is a controlling step for PAHs and particle growth and it was modeled considering both propargyl recombination and the C4 route. PAHs formation was modeled by both the hydrogen abstraction acetylene addition (HACA) and the resonantly stabilized free radical (RSFR) mechanisms. The molecular growth of PAHs was followed punctually up to pyrene. The kinetic gas-phase mechanism, as described, consists of 460 reactions involving 120 species. Particle formation was approached with a multi sectional scheme which considers large molecules, clusters i.e., single particles and aggregates. For each class of particles, a discretization on carbon and hydrogen atoms (31 and 5 sections respectively) and both stable and radical form were considered. All the steps for particle growth and oxidation, including size and temperature dependent coagulation and oxidation induced fragmentation were considered. Extensive details and validation of the model can be found in previous papers[35,37,36].

Computations were carried out in a domain that takes into account the geometry of the burner channels. A typical grid size in the flame region being 0.1 mm radial by 0.5 mm axial was used. Finer grids did not appreciably change the results. All the species equations were solved simultaneously at each spatial location in turn by a modified Newton−Raphson scheme. Velocity and enthalpy employed a tridiagonal matrix form of solution. For a converged solution, the mean absolute residual for a species, normalized by the species maximum value, was typically of the order of 10^{-7}, and overall carbon element mass balance error was less than 0.05%. Binary diffusion coefficients of species in nitrogen were used and the gas viscosity was approximated as that for nitrogen at every temperature. Diffusivities of the sectional species were obtained from Stokes friction with Cunningham correction factors based on the Knudsen number. Thermophoretic flux was applied to all the sections. The enthalpies of the sectional species were made the same per unit mass as that for pyrene.

The energy equation was fully solved and temperature was calculated. Radiative transfer was modeled by the discrete transfer method. Radiation heat losses are strongly influenced by the absorption coefficients of all the species. The absorption constant was therefore set to a value previously found for soot species and kept constant in this paper[19,38]. In this particular flame, the amount of soot particles formed (peak and integrated value) was not as high as in other hydrocarbon flames hence the impact of radiation is less important.

2.4 Thermocouple measurements

In this work, 4 different type S thermocouples (TC S.A., Pt-Pt/10%Rh) were used (0.20, 0.35, 0.42, 0.50 mm wire diameter given by the manufacturer and 0.62, 1.01, 1.15, 1.27 mm bead diameter measured with a 5 μm sensitivity micrometer). These small sized twin bore ceramic probes (the round bead insulation being composed of recrystallized alumina rated to 1700 °C) have been sheathed with Alsint tubes so as to limit conduction issues. To further limit conduction losses, the thermocouples were chosen to have wire length-to-diameter ratio higher than 300[13]. No specific surface treatment was applied to keep the diameter of the junction bead to the minimum size and to minimize the flame perturbation and detection delay.

The thermocouples were inserted radially into the centerline of the flame at different HABs thanks to a motorized remote-controlled system allowing the automatic and reproducible insertion. The difference of electric potential was followed in real time. The thermocouple insertion and permanence in the flame parameters, displayed in table 1, were experimentally adjusted to minimize the flame perturbation during insertion by operating a Labview code specifically written for these experiments.

Angular speed (rpm)	60

Time step (ms)	2
Acquisition time (s)	90

Table 1: Thermocouple fast insertion parameters

3. Results and Discussion

The extrapolation method correction is based on the principle that the radiation losses are dependent on the emitting surface and therefore, the thinner the thermocouple the lower the radiative losses. By using thermocouples with different diameters *d*, the flame temperature corrected from the radiation loss can then be deduced from the extrapolation measurements at *d=0*, as $T_0 = T(d \rightarrow 0)$ where T is measured at the same position with different thermocouples and d is a typical thermocouple size parameter as discussed below[13,21,22]. In addition, the raw temperature measured by each thermocouple is affected by the exposition time to the flame environment $T = T(t)$ and the presence of soot at the insertion point potentially changes the thermal properties of the thermocouple[18,39]. All the corrections required to retrieve the flame temperature are discussed case by case in the following sections.

3.1 Transient regime

Figure 2 shows the time evolution of the recorded temperature $T(t)$ during the insertion of the 0.20 mm thermocouple in the centerline of the flame at 15, 40, 70, 90 and 100 mm HAB, which correspond to very different chemical environments. Below 40 mm HAB, no soot is detected by LII[27]. In this case, a fast increase of the measured temperature is observed, corresponding to the transient response time of the thermocouple[18] (estimated to be less than 2s in our case), followed by a stable plateau when thermal equilibrium is reached for $T(t \rightarrow \infty)$, defined as when temperature temporal gradient is less than 0.03 K/s. A very similar behavior is observed above 90 mm HAB. Although in this flame region a strong LII signal was detected, the mature and partially oxidized soot does not deposit on the thermocouple surface that remains pristine during the entire data acquisition process[20,39].

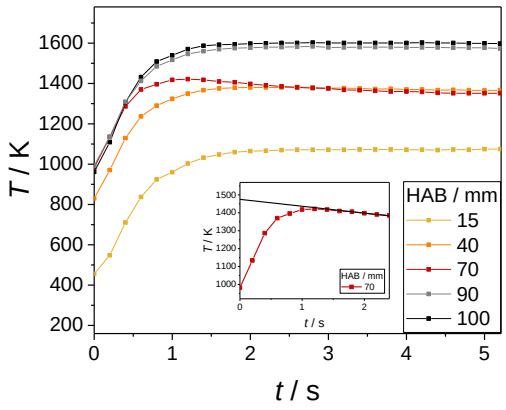

Fig. 2. T(t) recorded by the 0.20 mm S-type thermocouple at 15, 40, 70, 90 and 100 mm HAB.

3.2 Young soot correction

By contrast, in the flame region located between 55-80 mm HAB, soot and high mass hydrocarbons coexist as a high temperature aerosol[27] and are sufficiently reactive to quickly deposit on the thermocouple surface. This is reflected in the rapid and continuous decrease of $T(t)$ as the deposit builds up. This well-known issue, leading to the underestimation of the flame temperature measured in sooting flames in addition to the radiation losses, has been described by Mc Enally et al.[18], who notably showed that the errors in rapid insertion gas temperature measurements due to soot deposition depend linearly on the soot volume fraction and more strongly on the gas temperature. From our observations, the soot impact on temperature measurements with thermocouples appears also strongly correlated with its degree of maturity. Deposit of nascent soot emerging in the region 55-80 mm HAB are clearly present onto the thermocouple surface thus affecting temperature measurements. On the contrary mature soot formed upstream in the flame (above 80 mm) - as detected by optical techniques – does not remain on the thermocouple. Nascent particles, which are characterized by highest H/C ratio and aliphatic branching than mature soot [40,41] making these particles potentially stickier than carbonized and rigid mature soot. Oxidation of soot directly onto the thermocouple in higher regions of the flame, potentially even faster than oxidation occurring in gas phase, can also be responsible for these phenomena. Similar conclusions, were made by De Falco et al.[39], who correlated the degree of maturity with the emissivity of the deposit on the thermocouple junction and estimated the soot oxidation onto thermocouple junction.

Mc Enally et al.[18] estimated the error on gas temperature due to soot deposition by extrapolating the gas temperature back to the insertion time. It is to be noted that this method has been validated for relatively mild soot deposition corresponding to soot volume fractions lower than 50 ppm, which is far above the soot mole fraction expected in our flame (less than 300 ppb) [42,43]. As illustrated in the inset of fig.2 for 70 mm

HAB, this procedure was also used here to determine the corrected temperature from the soot deposit on the thermocouples in the 55-80 mm HAB range.

3.3 Radiative losses

The extrapolation method to correct for the radiative losses was applied to selected HABs at which the soot deposition rate on the thermocouples was verified to be negligible. This point was attested by the fast reaching of a stable temperature plateau as discussed above. $T(t\rightarrow\infty, d)$ was then measured as a function of a characteristic dimension of the junction d. The obtained data for different wire diameters at different HABs in the flame are reported in fig. 3.

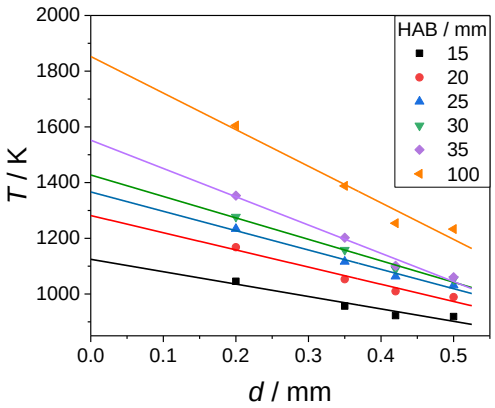

Fig.3. $T(t\rightarrow\infty, d)$ recorded for each of the 4 thermocouples at 15, 20, 25, 30 and 35 mm HAB and linear fit with extrapolation to obtain the temperature at zero wire diameter $T_0 = T(t\rightarrow\infty, d \rightarrow 0)$.

The wire diameter of the thermocouple was used as the independent variable rather than the bead diameter characterizing the thermocouple junction as sometimes found in the literature. Indeed, bead size correlations tend to be valid for approximately spherical beads much larger than the wire diameter[44,45]. In case of a small bead size relative to the wire diameter as in this work, the wires are rapidly heated by thermal conduction so that the presence of the bead is only a minor perturbation of the local temperature measurement at the junction, and the junction temperature is controlled primarily by heat transfer to the adjacent wires rather than to the junction[45].

Although higher degree polynomial functions are sometimes used[21,22,25], in this work, linear regressions are found to be the best fitting functions for $T(t\rightarrow\infty, d)$[14,15,46]. In fact, at every HAB, $T(t\rightarrow\infty, d)$ increases as the wire diameter decreases, consistently with the reduction of the impact of radiative heat losses on the temperature measurement. The reasons for this behavior are not clear yet, however we note that polynomial

functions are often used when an important dispersion of the experimental data is found or in case of long acquisition times to reach a stable reading are needed, potentially indicating additional effects other than radiation losses not considered in the analysis of the data.

Data and correlations reported in Fig.3 enable to define the calibration curve of each thermocouple, relating the measured raw temperatures to the corrected flame temperature T_0 from the radiation heat loss. Hence, from the linear extrapolations of the raw temperatures reported in fig.3 to zero wire diameter, it is possible to determine the value of the temperatures T_0 corresponding to the flame temperature values without radiation for each HAB and for each thermocouple.

3.4 Validation of the extrapolation method for flame studies

In order to setup the protocol for the determination of the temperature profiles in sooting flames, analysis of measurements in sooting flame region is reported. Figure 4 shows that, in the absence of soot deposition on the thermocouple surface, the measured temperature at thermal equilibrium corrected for radiation losses $T_0 = T(t\rightarrow\infty, d \rightarrow 0)$ is linearly correlated (R^2 >0.97) to the raw output of each thermocouple over the whole range of the flame temperatures.

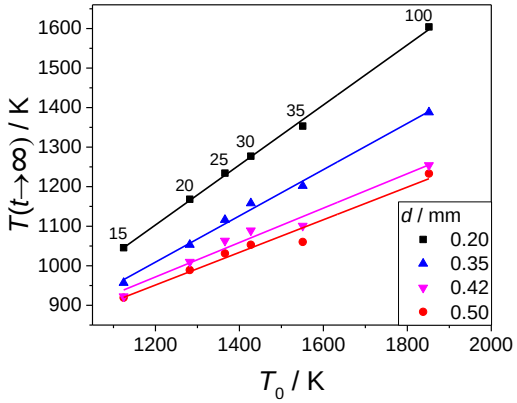

Fig. 4: Linear fit (calibration) of the measured temperature $T(t\rightarrow\infty)$ against the corrected temperature T_0 in the flame regions characterized by the absence of soot interference with the measurements (15, 20, 25, 30, 35 and 100 mm HAB).

Fig. 4 also shows that the radiation losses increase as the flame temperature increases (the thicker the thermocouple, the lower the measured raw temperature), leading to underestimations as high as 200K for a flame temperature in the order of 1600K. These values are in good agreement with previous temperature determinations relying on physical models for the estimation of the thermocouple radiation losses[14,15,40].

To finalize the validation of the extrapolation method for flame studies, the raw temperature profile of the flame along the vertical central axis was measured with the thinnest thermocouple (0.2 mm). This thermocouple was preferentially used to limit the impact of the radiative losses and flame perturbation and to maximize the spatial resolution of the measurements.

As discussed above, due to the high deposition rate of soot in the region 55-80 mm HAB, the thermocouples do not reach thermal equilibrium at these HABs. In order to find out the "soot-free" value of the raw temperatures in this case, the procedure proposed by McEnally et al.[18] discussed above was applied. To give an estimation of the correction provided by the use of the McEnally's method, we report in fig.4 for the region 55-80 mm HAB the peak temperature values quickly reached after the thermocouple insertion in the flame (corresponding to the peak value around 1s for the case illustrated in the inset of fig. 2). Hence the raw temperature profile reported in fig. 5 correspond to the $T(t\rightarrow\infty)$ temperatures, excepted in the zone 55-80 mm where we reported the measured quickly reached peak temperature values.

The final corrected temperature profile obtained by using to the calibration curve reported in fig.4 is compared in fig.5 to the temperature profiles obtained by OH and NO LIF thermometry and to the calculated profile. Uncertainties are estimated in the order of ±50 K for the temperature measurements using the 0.2 mm wire thermocouple over the temperature range from 1100 to 1800K.

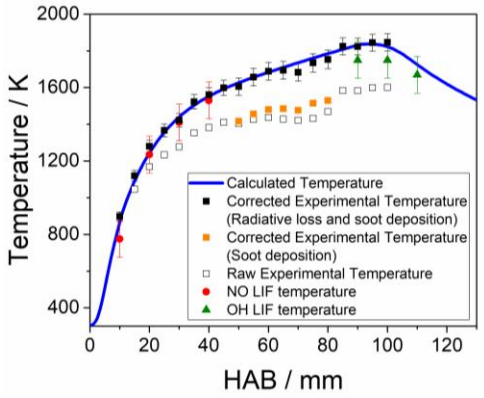

Fig. 5: Temperature profiles determined in the methane diffusion flame along the vertical central axis using the thermocouple methodology and compared with the calculated profile and OH / NO LIF thermometry.

As shown in fig. 5, the corrected temperature profile T_0, the LIF thermometry data and the calculated temperature profile are in excellent agreement, therefore validating the use of the extrapolation method for the temperature profile determination corrected from the radiation losses.

Consistently to the theory of radiation losses, the raw thermocouple output clearly appears below the corrected data, the difference gradually increasing with the temperature. The ditch in the raw thermocouple

output at 55-80 mm HAB due to the soot deposition on the thermocouple surface almost completely disappears after application of McEnally's correction. The difference between raw and corrected temperature is found in the order of 10-50K depending on the HAB, consistently with the values reported by McEnally in their original work[18]. Taking into account the weak correction allows to get a final perfect match of the experimental data with the reference temperature profiles. However, even in the sooting part of the flame, the dominant bias on the temperature measurement which appears very well corrected by our proposed methodology, clearly remains the radiation losses that lead to underestimations of the temperature in the order of 200K.

Radial profiles were also investigated to test the method with higher temperature gradients. To this aim we determined the radial temperature profiles for two different HABs in the sooting region of the flame and applied the same methodology as described above to obtain the corrected temperature profiles from both radiation losses et soot deposition. The results of these measurements and corresponding simulated temperature profiles are shown in fig.6.

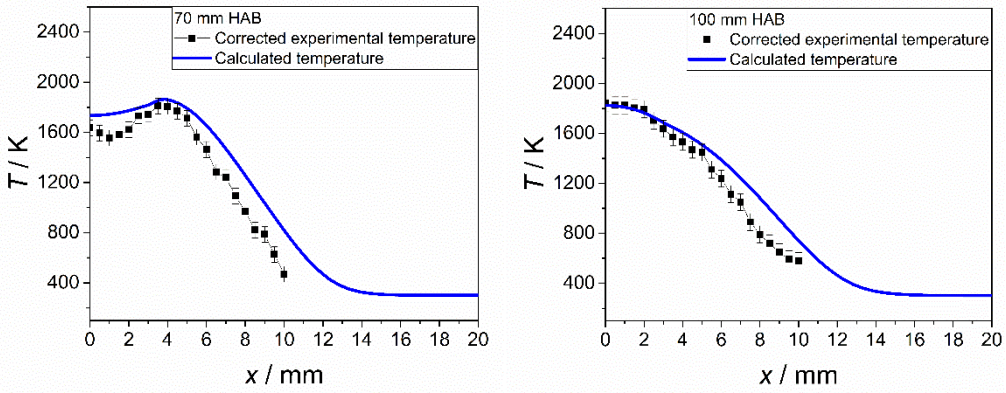

Fig. 6: Radial temperature profiles determined in the sooting region of the flame for two different HABs using the thermocouple methodology and compared with the calculated profiles

As can be seen, the comparison between the experimental and simulated profiles still highlights a very good agreement. Notably the experimental and simulated peak temperature obtained for each HAB shows an excellent concordance while the shape of the experimental profiles are well reproduced by the simulation. Our measurements highlight that the spatial resolution of the thermocouple method appears adequate for the determination of temperature profiles with gradients around 500K/mm. Moreover, it can be seen that the experimental measurements might even provide a better description of the radial temperature profile than the model at some locations, enabling for instance to reveal the slight curved shape of the profile between 0 and 2 mm at 70 mm HAB not captured by the model. Finally, a slight drift of the simulated profiles regarded to the experimental one is systematically observed at the edge of the flame for both HABs. These slight

discrepancies are likely related to the choice of boundary conditions applied to the model, particularly the heat exchange between the tip of the burner and the flame itself (actually neglected).

Hence, this work demonstrates the capability of this thermocouple method to easily access to accurate temperature measurements in harsh environments characterized by high temperature gradients. The reported work clearly highlights that the impact of the radiation losses appears to be very well corrected by the extrapolation method which allows a fast and accurate determination of the temperature profile all along the flame height including in presence of soot.

Currently, the technique has been demonstrated to be a valuable and simple alternative method for the determination of accurate temperature for the specific case of laminar and potentially sooting flames. We did not check the validity of the method for more complex environments as turbulent flames. One of the main limitation in that context concerns the transient time required by the thermocouple to reach its peak temperature value. Depending on this value, temperature evolutions of turbulent systems might or not be capture by the thermocouple. In our case, the transient time was estimated around 1 s which is definitely too slow to allow the capture of turbulent events. However, Ren et al[24] succeed to record to record temperature evolutions resolving very short timescales in a turbulent ethylene flame with much thinner thermocouples as we used, letting hope that our methodology implemented with thermocouple characterized by thinner diameter and faster transient times might be envisaged for turbulent applications.

4. Conclusions

This work reports the implementation and the validation of the extrapolation method for thermocouple temperature measurements corrected from the radiation losses in sooting flames. All the measurements were carried out in a laminar diffusion sooting flame of methane. The method relies on the proportionality of the radiation losses to the size of the thermocouple and thus the flame temperature can be obtained by extrapolation to zero diameter. In this work, the measured raw temperature is shown to be linearly correlated to the wire diameter of the thermocouples. By applying this procedure for selected HABs characterized by different flame temperatures, it is therefore possible to build calibration curves for selected thermocouples that relate the raw measured temperature to the flame temperature corrected from the radiation losses. This linearity has at least one important practical consequence, as in principle only two thermocouples having different diameters are needed for a reliable flame temperature measurement, and could therefore help the development of fast and cheap sensors for either laboratory or large-scale applications.

In terms of accuracy, since the thermocouples located in the sooting region of the flame did not reach thermal equilibrium due to the high soot deposition rate, a specific procedure proposed in the literature[18] had to be applied to determine the “soot-free” value of the raw temperatures. This correction has been found

here to be in the order of 10-50K, while the impact of radiative losses has been determined to be as high as to 200K. Finally, the comparison of the determined profile by the extrapolation method with reference temperature profiles obtained by LIF thermometry and numerical simulation show excellent agreements.

These results overall demonstrate that the extrapolation method is an efficient and fast method to determine temperature profiles in flames with high accuracy, even in presence of soot particles. The use of this method, allowing the very fast calibration of thermocouples, appears very simple to implement in comparison to the electrical compensation method or the complex estimation of the radiation loss of the thermocouple.

This proposed methodology could be advantageously used for temperature measurements either for laboratory flames studies or potentially more hostile environments where the radiation losses estimations are quite complex to determine.

Acknowledgements

This work was supported by the Agence Nationale de la Recherche through the LABEX CAPPA (ANR-11-LABX-0005), the Région Hauts-de-France, the Ministère de l'Enseignement Supérieur et de la Recherche (CPER Climibio) and the European Fund for Regional Economic Development.

References

1 C. R. Shaddix, *Correcting thermocouple measurements for radiation loss: A critical review*, American Society of Mechanical Engineers, New York, NY (US), 1999.
2 A. C. Eckbreth, *Laser Diagnostics for Combustion Temperature and Species*, Second Edition. Combustion Science and Technology Book Series, Volume 3. Gordon and Breach Publishers., 1996.
3 D. R. Snelling, K. A. Thomson, G. J. Smallwood, Ö. L. Gülder, E. J. Weckman and R. A. Fraser, Spectrally Resolved Measurement of Flame Radiation to Determine Soot Temperature and Concentration, *AIAA Journal*, 2002, **40**, 1789–1795.
4 J. Yon, J. J. Cruz, F. Escudero, J. Morán, F. Liu and A. Fuentes, Revealing soot maturity based on multi-wavelength absorption/emission measurements in laminar axisymmetric coflow ethylene diffusion flames, *Combustion and Flame*, 2021, **227**, 147–161.
5 M. R. Kholghy, Y. Afarin, A. D. Sediako, J. Barba, M. Lapuerta, C. Chu, J. Weingarten, B. Borshanpour, V. Chernov and M. J. Thomson, Comparison of multiple diagnostic techniques to study soot formation and morphology in a diffusion flame, *Combustion and Flame*, 2017, **176**, 567–583.
6 W. G. Bessler and C. Schulz, Quantitative multi-line NO-LIF temperature imaging, *Appl Phys B*, 2004, **78**, 519–533.
7 K. J. Rensberger, J. B. Jeffries, R. A. Copeland, K. Kohse-Höinghaus, M. L. Wise and D. R. Crosley, Laser-induced fluorescence determination of temperatures in low pressure flames, *Appl. Opt., AO*, 1989, **28**, 3556–3566.
8 A. T. Hartlieb, B. Atakan and K. Kohse-Höinghaus, Temperature measurement in fuel-rich non-sooting low-pressure hydrocarbon flames, *Appl Phys B*, 2000, **70**, 435–445.

9 I. Rahinov, A. Goldman and S. Cheskis, Absorption spectroscopy diagnostics of amidogen in ammonia-doped methane/air flames, *Combustion and Flame*, 2006, **145**, 105–116.
10 K. K. Foo, N. Lamoureux, A. Cessou, C. Lacour and P. Desgroux, The accuracy and precision of multi-line NO-LIF thermometry in a wide range of pressures and temperatures, *Journal of Quantitative Spectroscopy and Radiative Transfer*, 2020, **255**, 107257.
11 R. D. Hancock, K. E. Bertagnolli and R. P. Lucht, Nitrogen and hydrogen CARS temperature measurements in a hydrogen/air flame using a near-adiabatic flat-flame burner, *Combustion and Flame*, 1997, **109**, 323–331.
12 M. V. Heitor and A. L. N. Moreira, Thermocouples and sample probes for combustion studies, *Progress in Energy and Combustion Science*, 1993, **19**, 259–278.
13 D. Bradley and K. J. Matthews, Measurement of High Gas Temperatures with Fine Wire Thermocouples, *Journal of Mechanical Engineering Science*, 1968, **10**, 299–305.
14 V. Hindasageri, R. P. Vedula and S. V. Prabhu, Thermocouple error correction for measuring the flame temperature with determination of emissivity and heat transfer coefficient, *Review of Scientific Instruments*, 2013, **84**, 024902.
15 R. Lemaire and S. Menanteau, Assessment of radiation correction methods for bare bead thermocouples in a combustion environment, *International Journal of Thermal Sciences*, 2017, **122**, 186–200.
16 J. KENT, A Noncatalytic Coating for Platinum-Rhodium Thermcouples, *Combustion and Flame*, 1970, **14**, 279–282.
17 R. C. Peterson and N. M. Laurendeau, The emittance of yttrium-beryllium oxide thermocouple coating, *Combustion and Flame*, 1985, **60**, 279–284.
18 C. S. McEnally, Ü. Ö. Köylü, L. D. Pfefferle and D. E. Rosner, Soot volume fraction and temperature measurements in laminar nonpremixed flames using thermocouples, *Combustion and Flame*, 1997, **109**, 701–720.
19 G. De Falco, M. Sirignano, M. Commodo, L. Merotto, F. Migliorini, R. Dondè, S. De Iuliis, P. Minutolo and A. D'Anna, Experimental and numerical study of soot formation and evolution in co-flow laminar partially premixed flames, *Fuel*, 2018, **220**, 396–402.
20 G. De Falco, M. Commodo, A. D'Anna and P. Minutolo, The evolution of soot particles in premixed and diffusion flames by thermophoretic particle densitometry, *Proc. Comb. Inst.*, 2017, **36**, 763–770.
21 G. E. Daniels, Measurement of Gas Temperature and the Radiation Compensating Thermocouple, *Journal of Applied Meteorology and Climatology*, 1968, **7**, 1026–1035.
22 E. L. Nichols, On the Temperature of the Acetylene Flame, *Phys. Rev. (Series I)*, 1900, **10**, 234–252.
23 K. Seshadri and D. E. Rosner, Optical methods and results of dew point and deposition rate measurements in salt/ash-containing combustion gases—B2O3(I) deposition rates by interference methods and comparisons with theory, *AIChE Journal*, 1984, **30**, 187–196.
24 X. Ren, D. Zeng, Y. Wang, G. Xiong, G. Agarwal and M. Gollner, Temperature measurement of a turbulent buoyant ethylene diffusion flame using a dual-thermocouple technique, *Fire Safety Journal*, 2021, **120**, 103061.
25 A. Ergut and Y. Levendis, American Society of Mechanical Engineers Digital Collection, 2008, pp. 397–403.
26 A. Faccinetto, C. Irimiea, P. Minutolo, M. Commodo, A. D'Anna, N. Nuns, Y. Carpentier, C. Pirim, P. Desgroux, C. Focsa and X. Mercier, Evidence on the formation of dimers of polycyclic aromatic hydrocarbons in a laminar diffusion flame, *Commun. Chem.*, 2020, **3**, 1–8.
27 X. Mercier, O. Carrivain, C. Irimiea, A. Faccinetto and E. Therssen, Dimers of polycyclic aromatic hydrocarbons: the missing pieces in the soot formation process, *Phys. Chem. Chem. Phys.*, 2019, **21**, 8282–8294.
28 I. S. McDermid and J. B. Laudenslager, Radiative lifetimes and electronic quenching rate constants for single-photon-excited rotational levels of no (A2Σ+, ν′ = 0), *Journal of Quantitative Spectroscopy and Radiative Transfer*, 1982, **27**, 483–492.

29 G. F. Nutt, S. C. Haydon and A. I. McIntosh, Measurement of electronic quenching rates in nitric oxide using two-photon spectroscopy, *Chemical Physics Letters*, 1979, **62**, 402–404.
30 H. Zacharias, J. B. Halpern and K. H. Welge, Two-photon excitation of NO(A2Σ+; ν′ = 0,1,2) and radiation lifetime and quenching measurements, *Chemical Physics Letters*, 1976, **43**, 41–44.
31 K. Kohse-Höinghaus, Laser techniques for the quantitative detection of reactive intermediates in combustion systems, *Progress in Energy and Combustion Science*, 1994, **20**, 203–279.
32 X. Mercier, L. Pillier, A. El Bakali, M. Carlier, J.-F. Pauwels and P. Desgroux, NO reburning study based on species quantification obtained by coupling LIF and cavity ring-down spectroscopy, *Faraday Discussions*, 2001, **119**, 305–319.
33 A. Goldman and S. Cheskis, Intracavity laser absorption spectroscopy of sooting acetylene/air flames, *Appl. Phys. B*, 2008, **92**, 281.
34 J. Luque and D. R. Crosley, LIFBASE: Database and Spectral Simulation Program (Version 1.5), *SRI International Report MP 99-009*.
35 A. D'Anna, M. Sirignano and J. Kent, A model of particle nucleation in premixed ethylene flames, *Combustion and Flame*, 2010, **157**, 2106–2115.
36 M. Sirignano, J. Kent and A. D'Anna, Modeling Formation and Oxidation of Soot in Nonpremixed Flames, *Energy & Fuels*, 2013, **27**, 2303–2315.
37 M. Sirignano, J. Kent and A. D'Anna, Detailed modeling of size distribution functions and hydrogen content in combustion-formed particles, *Combustion and Flame*, 2010, **157**, 1211–1219.
38 M. Sirignano, G. De Falco, M. Commodo, P. Minutolo, C. Tregambi, R. Solimene and P. Salatino, Experimental and numerical study of a hybrid solar-combustor system for energy efficiency increasing, *Fuel*, 2020, **263**, 116732.
39 G. De Falco, G. Moggia, M. Sirignano, M. Commodo, P. Minutolo and A. D'Anna, Exploring Soot Particle Concentration and Emissivity by Transient Thermocouples Measurements in Laminar Partially Premixed Coflow Flames, *Energies*, 2017, **10**, 232.
40 M. R. Kholghy, A. Veshkini and M. J. Thomson, The core–shell internal nanostructure of soot – A criterion to model soot maturity, *Carbon*, 2016, **100**, 508–536.
41 B. Öktem, M. P. Tolocka, B. Zhao, H. Wang and M. V. Johnston, Chemical species associated with the early stage of soot growth in a laminar premixed ethylene-oxygen-argon flame, *Combustion and Flame*, 2005, **142**, 364–373.
42 B. Tian, Y. Gao, S. Balusamy and S. Hochgreb, High spatial resolution laser cavity extinction and laser-induced incandescence in low-soot-producing flames, *Appl. Phys. B*, 2015, **120**, 469–487.
43 B. Tian, Y. Gao, C. Zhang and S. Hochgreb, Soot measurement in diluted methane diffusion flames by multi-pass extinction and laser-induced incandescence, *Combustion and Flame*, 2018, **192**, 224–237.
44 W. M. Pitts, E. Braun, R. D. Peacock, H. E. Mitler, E. L. Johnsson, P. A. Reneke and L. G. Blevins, Temperature Uncertainties for Bare-Bead and Aspirated Thermocouple Measurements in Fire Environments, *ASTM Special Technical Publication*, 2002, **1427**, 3–15.
45 A. N. Hayhurst and D. B. Kittelson, Heat and mass transfer considerations in the use of electrically heated thermocouples of iridium versus an iridiumrhodium alloy in atmospheric pressure flames, *Combustion and Flame*, 1977, **28**, 301–317.
46 J. D. Walker and B. J. Stocks, Thermocouple errors in forest fire research, *Fire Technol*, 1968, **4**, 59–62.